Assessment of Histone H2AX Phosphorylation Induced by DNA Topoisomerase I and II Inhibitors Topotecan and Mitoxantrone and by the DNA Cross-Linking Agent Cisplatin

ARTICLE *in* CYTOMETRY PART A · APRIL 2004

Impact Factor: 2.93 · DOI: 10.1002/cyto.a.20018 · Source: PubMed

6 AUTHORS, INCLUDING:

Xuan Huang
Northwest University
31 PUBLICATIONS **1,593** CITATIONS
SEE PROFILE

Ed Luther
Northeastern University
31 PUBLICATIONS **1,520** CITATIONS
SEE PROFILE

Elena Holden
Thorlabs, Inc.
12 PUBLICATIONS **294** CITATIONS
SEE PROFILE

Zbigniew Darzynkiewicz
New York Medical College
265 PUBLICATIONS **8,456** CITATIONS
SEE PROFILE

Cytometry Part A 58A:99–110 (2004)

Rapid Communication

Assessment of Histone H2AX Phosphorylation Induced by DNA Topoisomerase I and II Inhibitors Topotecan and Mitoxantrone and by the DNA Cross-Linking Agent Cisplatin

Xuan Huang,[1] Masaki Okafuji,[1,2] Frank Traganos,[1] Ed Luther,[3] Elena Holden,[3] and Zbigniew Darzynkiewicz[1]*

[1]Brander Cancer Research Institute, New York Medical College, Valhalla, New York
[2]Department of Oral and Maxillofacial Surgery, Yamaguchi University, School of Medicine, Ube, Japan
[3]CompuCyte Corporation, Cambridge, Massachusetts

Received 22 January 2004; Revision Received 22 January 2004; Accepted 23 January 2004

Background: DNA double-strand breaks (DSBs) in chromatin, whether induced by radiation, antitumor drugs, or by apoptosis-associated (AA) DNA fragmentation, provide a signal for histone H2AX phosphorylation on Ser-139; the phosphorylated H2AX is denoted γH2AX. The intensity of immunofluorescence (IF) of γH2AX was reported to reveal the frequency of DSBs in chromatin induced by radiation or by DNA topoisomerase I (topo 1) and II (topo 2) inhibitors. The purpose of this study was to further characterize the drug-induced (DI) IF of γH2AX, and in particular to distinguish it from AA γH2AX IF triggered by DNA breaks that occur in the course of AA DNA fragmentation.

Methods: HL-60 cells in cultures were treated with topotecan (TPT), mitoxantrone (MTX), or with DNA cross-linking drug cisplatin (CP); using multiparameter flow and laser-scanning cytometry, induction of γH2AX was correlated with: 1) caspase-3 activation; 2) chromatin condensation, 3) cell cycle phase, and 4) AA DNA fragmentation. The intensity of γH2AX IF was compensated for by an increase in histone/DNA content, which doubles during the cell cycle, and for the "programmed" H2AX phosphorylation, which occurs in untreated cells.

Results: In cells treated with TPT or MTX, the increase in DI-γH2AX IF peaked at 1.5 or 2 h, and was maximal in S- or G_1-phase cells, respectively, for each drug. In cells treated with CP, compared with TPT, the γH2AX IF was less intense, peaked later (3 h) and showed no cell cycle–phase specificity. In the presence of phosphatase inhibitor calyculin A, a continuous increase in the TPT-induced γH2AX IF was still seen past 1.5 h, and after 3 h γH2AX IF was 2.7- to 3.4-fold higher than in the absence of the inhibitor. The AA γH2AX IF was distinguished from the DI-γH2AX IF by: 1) its greater intensity; 2) its prevention by caspase inhibitor zVAD-FMK; and 3) the concurrent activation of caspase-3 in the same cells. A decrease in AA γH2AX IF coinciding with AA chromatin condensation was seen in the late stages of apoptosis.

Conclusions: Multiparameter analysis of γH2AX IF, caspase-3 activation, cellular DNA content, and chromatin condensation allowed us to distinguish the DI from AA H2AX phosphorylation and relate them to the cell cycle phase and stage of apoptosis. With a comparable degree of ds DNA breaks, the cells arrested at the G_1 or G_2/M checkpoint were less prone to undergo apoptosis than the cells replicating DNA. H2AX phosphorylation seen in CP-treated cells may be associated with DNA repair that involves nucleotide excision repair (NER) and nonhomologous end joining (NHEJ). When the primary drug-induced lesions do not involve ds DNA breaks, but ds DNA breaks are formed during DNA repair, as in the case of CP, analysis of H2AX phosphorylation may reflect extent of the repair process. © 2004 Wiley-Liss, Inc.

Key terms: DNA repair; nucleotide excision repair; DNA replication; DNA breaks; dosimetry; cell cycle; apoptosis; S phase; chromatin; laser scanning cytometry; iCyte

*Correspondence to: Dr. Z. Darzynkiewicz, Brander Cancer Research Institute at NYMC, 19 Bradhurst Avenue, Suite 2400, Hawthorne, NY 10532.
Contract grant sponsor: NCI; Contract grant number: CA 28704.
E-mail: darzynk@nymc.edu

Published online 5 March 2004 in Wiley InterScience (www.interscience.wiley.com).
DOI: 10.1002/cyto.a.20018

Histone H2AX is one of the heteromorphous variants of family of at least eight protein species of the nucleosome core histone H2A (1–3). Induction of DNA double strand breaks (DSBs) in live cells triggers its phosphorylation (4,5). The phosphorylation is mediated by ATM- (4–7), ATR- (8), and/or DNA-dependent protein kinase (DNA-PK) (9), affects H2AX molecules flanking the DSBs in chromatin, and occurs on Ser 139 (4,5) at the C terminus. The phosphorylated form of H2AX has been defined as γH2AX (10). Shortly after induction of DSBs by ionizing radiation, the appearance of γH2AX in chromatin can be detected immunocytochemically in the form of discrete nuclear foci (5,10), each focus being presumed to represent a single DSB (5). The frequency of foci per nucleus, thus, is considered to reflect the incidence of DSBs. Checkpoint and DNA repair proteins such as Rad50, Rad51, and Brca1 colocalize with γH2AX (11). In addition, the translocation of the p53 binding protein 1 (53BP1) to irradiation-induced foci is mediated by H2AX (7–9). However, it was recently shown that while the migration of repair and signaling proteins to DSBs is not abrogated in H2AX (−/−) cells, these proteins fail to form irradiation-induced foci (12). The loss of H2AX in mice leads to genomic instability (13). The H2AX −/− mice are radiation sensitive, growth retarded, and immune deficient (13). H2AX haploinsufficiency compromises genetic integrity, and in the absence of p53, enhances susceptibility to cancer (14). H2AX, thus, appears to be a caretaker of genomic integrity that requires the function of both alleles for optimal protection against carcinogenesis (15).

H2AX is also phosphorylated in healthy, nontreated cells, in response to the formation of DSBs occurring in V(D)J and class-switch recombination during immune system development (16–20), as well as in association with DNA replication (21) in S phase cells. Likewise, DSBs generated in the course of DNA fragmentation in apoptotic cells also induce H2AX phosphorylation (21).

The intensity of γH2AX immunofluorescence (IF) measured by cytometry was reported to correlate with the dose of ionizing irradiation used to induce DSBs (21). However, since normal cells, particularly the cells replicating DNA, express γH2AX (21,22), to obtain a stoichiometric relationship between DSBs and the intensity of γH2AX IF resulting from drug-induced (DI) DNA damage, compensation must be used to account for the extent of this "programmed" H2AX phosphorylation. Following compensation, the γH2AX IF measured by cytometry offers a sensitive and convenient means to detect and measure DSBs in individual cells (21,23), and has been proposed as a surrogate for cell killing in viability tests for drugs that generate DSBs (24). These elegant studies by MacPhail et al. (21,23) and Banath and Olive (24), provided evidence that DSBs induced by radiation can be detected and conveniently measured using multiparameter flow and image cytometry of γH2AX IF.

Inhibitors of DNA topoisomerase I and II (topo1 and topo2) are among the most clinically effective antitumor drugs. They work by stabilizing otherwise transient "cleavable complexes" formed between topo1 or topo2 and DNA (25). In DNA replicating cells this leads to the collision between the progressing DNA replication fork and the stabilized complex, and in turn, to conversion of the complex into secondary lesions that consist of DSBs (25). Collisions with the cleavable complexes also occur during transcription, between the progressing RNA polymerase molecule and the inhibitor-stabilized topo1 or topo2 cleavable complex located on the template strand within the DNA region being transcribed (26). The RNA polymerase collisions, similar to the collisions of the DNA replication fork, are also converted into DSBs (27). In both instances, it is presumed that the secondary DSB lesions are recognized by the cell as lethal and that they trigger apoptosis (25–27). Predominantly S-phase cells undergo apoptosis upon exposure to topo1 or topo2 inhibitors (28–30). In contrast to topo inhibitors, which generate DSBs, cisplatin (CP) induces primarily DNA intrastrand cross-links. Single-strand DNA breaks, however, appear during the nucleotide excision repair of the CP-induced lesions (31,32).

In a previous study (33), we reported that H2AX was phosphorylated in response to DNA damage induced by topo1 (camptothecin [CPT] and topotecan [TPT]) and topo2 (mitoxantrone [MTX]) inhibitors. Furthermore, using multiparameter cytometry, we correlated the induction of γH2AX with cell cycle position. We also observed that induction of γH2AX in response to DNA lesions preceded apoptosis, as detected by caspase-3 activation and DNA fragmentation (33). The aim of the present study was to develop the means to identify the DI H2AX phosphorylation from the subsequent, apoptosis-associated (AA) phosphorylation of H2AX, which occurs in response to DNA fragmentation during apoptosis. Analyzing activation of caspase-3, the enzyme that activates the DNase that fragments DNA during apoptosis (34), along with induction of γH2AX, and correlating these events with cell cycle position and chromatin condensation (33), all measured by laser scanning cytometry (LSC) (36,37), or iCyte, the more advanced version of LSC, we have been able to characterize the DI γH2AX IF and AA γH2AX IF in HL-60 cells treated with TPT, MTX, or CP.

MATERIALS AND METHODS

Cells and Cell Treatment

Human promyelocytic leukemic HL-60 cells were obtained from American Type Culture Collection (ATCC, Rockville, MD). The cells were grown in 25 ml FALCON flasks (Becton Dickinson Co., Franklin Lakes, NJ) in RPMI 1640, supplemented with 10% fetal calf serum, 100 units/ml penicillin, 100 μg/ml streptomycin, and 2 mM L-glutamine (all from GIBCO/BRL Life Technologies, Inc., Grand Island, NY) at 37.5°C in an atmosphere of 5% CO_2 in air. At the onset of the experiments, there were fewer than 5×10^5 cells per ml in culture and the cells were at an exponential and asynchronous phase of growth. To induce apoptosis, the cultures were treated with various concentrations of topotecan (TPT), an analog of campto-

thecin (CPT; Hycamptin, Merck Pharmaceutical Co., Rahway, NJ), mitoxantrone (MTX, American Cyanamid, Pearl River, NY), or cisplatin (CP, American Pharmaceutical Partners, Inc., Los Angeles, CA) as described in the figure 1–9 legends. Control cultures were treated with the equivalent volumes of dimethylsulfoxide (DMSO, Sigma, St. Louis, MO), which were used to prepare stock solutions of the drugs. Some cultures were also treated with 50 μM pan-caspase inhibitor zVAD-FMK (Enzyme Systems Products, Livermore, CA), or with 10 nM calyculin A (Biomol, Plymouth, PA). Details are provided in the figure 1–9 legends.

Detection of Histone γH2AX and of Caspase-3 Activation: Samples Prepared for FCM

Cells were treated with different concentration of drugs, rinsed with PBS, and then fixed in suspension in 1% methanol-free formaldehyde (Polysciences, Warrington, PA) in PBS at 0°C for 15 min, then resuspended in 70% ethanol for at least 2 h at –20°C. The cells were then washed twice in PBS and suspended in 0.2% Triton X-100 (Sigma) in a 1% (w/v) solution of BSA (Sigma) in PBS for 30 min to suppress nonspecific Ab binding. The cells were centrifuged again (200 *g*, 5 min) and the cell pellet was suspended in 100 μl of 1% BSA containing either 1:800 diluted anti-histone γH2AX polyclonal Ab (Trevigen, Gaithersburg, MD) or 1:100 dilution of anti-cleaved (activated) caspase-3 polyclonal Ab (Cell Signaling Technology, Beverly, MA). The cells were then incubated overnight at 4°C, washed twice with PBS, and resuspended in 100 μl of 1:30 diluted FITC-conjugated F(ab′)2 fragment of swine anti-rabbit immunoglobulin (DAKO, Carpinteria, CA) for 30 min in room temperature in the dark. The cells were then counterstained with 5 μg/ml of PI (Molecular Probes, Eugene, OR) dissolved in PBS containing 100 μg/ml of DNase-free RNase A (Sigma), for 20 min at room temperature. Cellular fluorescence was measured using a FACScan flow cytometer (Becton-Dickinson).

Detection of Histone γH2AX and of Caspase-3 Activation: Samples Prepared for Analysis by Laser Scanning Cytometry (LSC) or iCyte

Cells were treated with drugs as described above, rinsed with PBS and then cytocentrifuged onto microscope slides. The slides were fixed in Coplin jars in 1% methanol-free formaldehyde in PBS at 0°C for 15 min then transferred to 70% ethanol for at least 2 h at –20°C. The slides were then rinsed twice in PBS and the cells were immersed in 0.2% Triton X-100 (Sigma) in a 1% (w/v) solution of PBS for 30 min. The cytocentrifuged cells were then incubated in 100 μl volume of 1% BSA containing 1:200 diluted anti-phospho-histone H2AX (Ser139) murine monoclonal Ab (Upstate, Lake Placid, NY) and a 1:100 dilution of anti-cleaved (activated) caspase-3 rabbit polyclonal Ab (Cell Signaling Technology, Beverly, MA) overnight at 4°C, washed twice with PBS, and then incubated in 100 μl of 1:100 diluted Alexa Fluor 633 conjugated F(ab′)2 fragment of goat anti-mouse IgG (H+L) (Molecular Probes, Eugene, OR) and 1:30 diluted FITC-conjugated F(ab′)2 fragment of swine anti-rabbit immunoglobulin (DAKO, Carpinteria, CA) for 30 min in room temperature in the dark. The cells were then counterstained with 1 μg/ml 4,6-diamidino-2-phenylindole (DAPI; Molecular Probes, Eugene, OR) in PBS for 5 min.

In Situ DNA Strand Break Labeling (TUNEL Assay)

Apoptosis of HL-60 cells was induced by incubation with 200 nM MTX, or 150 nM TPT or CPT for various lengths of time. The cells were then rinsed with PBS (200 *g*; 5 min), fixed in 1% methanol-free formaldehyde for 15 min at room temperature, and stored in 70% ethanol at –20°C for at least 2 h. The cells were then rinsed twice with PBS for 5 min. DNA strand break labeling (38) was performed using the APO-BRDU kit (39) provided by Phoenix Flow Systems (San Diego, CA). After washing with PBS, cells were stained with 5 μg/ml of PI dissolved in PBS containing 100 μg/ml of DNase-free RNase A, for 20 min.

Fluorescence Measurement

FCM. Cellular green (histone γH2AX, cleaved caspase 3, or BrdU)- and red (PI)- fluorescence was measured using a FACScan (Becton Dickinson, San Jose, CA) with the standard emission filters for green (FL1) and red (FL3) fluorescence as described (40).

LSC and iCyte. Cellular green (cleaved caspase 3), far red (histone γH2AX) and blue (DAPI) fluorescence emission was measured simultaneously in the same cells either using a laser scanning cytometer (LSC; CompuCyte, Cambridge, MA) (36,37), utilizing standard filter settings; fluorescence was excited with 488-nm argon ion, helium neon, and violet diode lasers, respectively. In some experiments the measurements were carried out using iCyte (CompuCyte), the more recent and advanced version of the laser scanning cytometer. The intensities of maximal pixel and integrated fluorescence were measured and recorded for each cell. At least 3,000 cells were measured per sample.

Quantitation of γH2AX IF

To compare the changes in γH2AX IF intensity, e.g., in relation to cell cycle phase or drug concentration, the mean γH2AX IF intensity (integral values of individual cells) was calculated per cell, in each phase of the cycle by gating G_1, S, and G_2/M cells based on differences in DNA content. The means of γH2AX IF for G_1, S, and G_2/M populations of untreated cells were then subtracted from the respective means of the drug-treated cells to obtain the DI differential γH2AX IF (Δ-γH2AX IF). The Δ-γH2AX IF is expressed as the percent of the mean γH2AX IF of the untreated cells, which were normalized per unit of DNA (see below), and serve as the "yardstick" for IF intensity. The data shown in the plots (Figs. 2 and 3), therefore, represent the percent-increase of the mean γH2AX IF in the drug-treated cells over the mean value of the "scheduled" γH2AX IF, calculated separately for each phase of the cell cycle. To compensate for the increase in DNA/histone content during the cell cycle progression, the

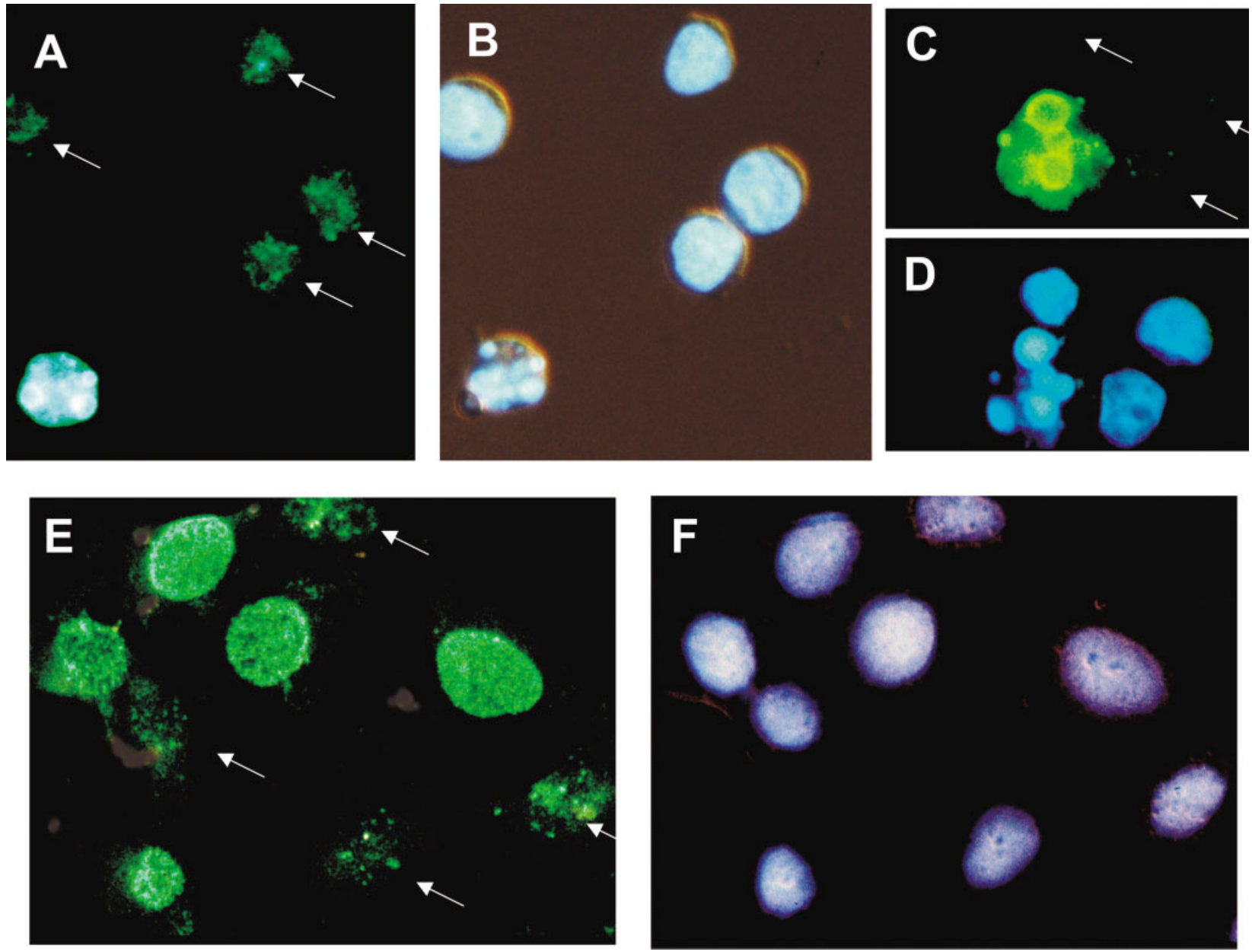

FIG. 1. γH2AX Ab immunofluorescence (**A**,**C**,**E**) and DAPI fluorescence (**B**,**D**,**F**) of HL-60 cells, untreated (A,B) and treated with 0.15 μM TPT (C–F).

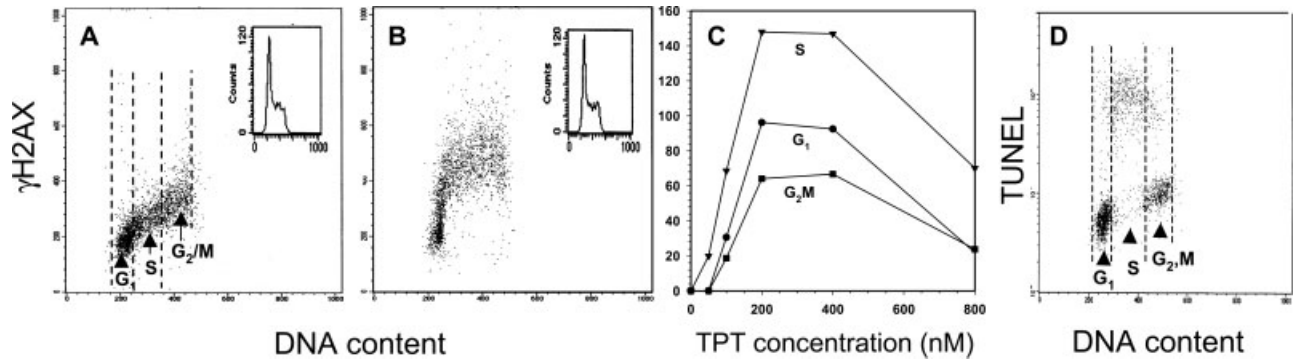

FIG. 2. Induction of γH2AX (**A–C**), and apoptosis (**D**) in HL-60 cells treated with TPT in relation to the cell cycle phase. Untreated (A) or treated with 0.15 μM TPT for 1.5 h HL-60 cells (B) were immunostained for γH2AX using indirect FITC-tagged Ab, and their DNA was counterstained with PI; the cell fluorescence was measured by flow cytometry. Note an increase in γH2AX IF occurring predominantly in S- and in a portion of the G_1- phase cells, after the treatment (B). The plot in C shows the percent increase in mean γH2AX IF of the cells treated with different concentration of TPT for 1.5 h, over the mean values of γH2AX IF of the untreated cells (Ctrl), in the respective phases of the cell cycle, compensated to account for the increased DNA/histone content in S- and G_2/M-, compared to G_1-, cells, as described in the text. The S-phase cells are preferentially undergoing apoptosis, as evidenced by the presence of TUNEL-positive cells with an S-DNA content. (D).

means of γH2AX IF for S and G_2/M of the untreated cells (used as the yardstick), as well as the means of Δ-γH2AX IF for S and G_2/M phase cells, were multiplied by 0.75 and 0.5, respectively. Thus, Δ-γH2AX IF compensated this way represents the increase in γH2AX IF intensity per unit of histone, presumed to reflect the increase in the degree of H2AX phosphorylation (independent of changes in histone/DNA content during the cycle or of differences in DNA ploidy) rather than the increase in total γH2AX content per cell.

Fluorescence Microscopy

Localization of γH2AX was determined by immunofluorescence analysis by using antibodies against phosphorylated histone H2AX. Untreated and TPT-treated HL-60 cells were cytocentrifuged onto slides and fixed in 1% methanol-free formaldehyde in PBS at 0°C for 15 min, then transferred to 70% ethanol for at least 2 h at –20°C. The slides were then rinsed twice in PBS and were treated with 0.1% Triton X-100 in PBS for 5 min on ice. After blocking with 1% BSA in PBS for 30 min, the cells were incubated in 1% BSA containing 1:800 diluted anti-histone γH2AX polyclonal Ab (Trevigen, Gaithersburg, MD) for 2 h at room temperature, washed twice with PBS, and then incubated in 1:30 diluted FITC-conjugated F(ab′)2 fragment of swine anti-rabbit immunoglobulin (DAKO, Carpinteria, CA) for 30 min at room temperature in the dark. The cells were then counterstained with 1μg/ml DAPI. Cellular morphology and fluorescence (Fig. 1) was examined under a Nikon Microphot FXA microscope, utilizing a 40× objective.

Each experiment was repeated at least three times.

RESULTS

Figure 1 illustrates labeling with γH2AX Ab of HL-60 cells, untreated (Fig. 1A and B) or treated with TPT for

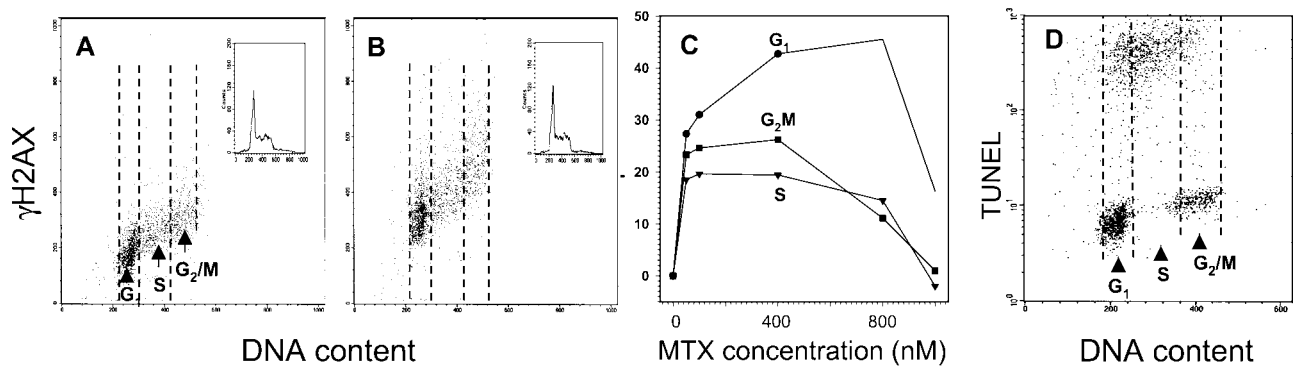

FIG. 3. Induction of γH2AX (**A–C**), and apoptosis (**D**) in HL-60 cells treated with MTX in relation to the cell cycle phase. Untreated (A) and treated with 0.15 μg/ml MTX for 2 h HL-60 cells (B) were immunostained for γH2AX and their DNA was counterstained with PI; the cell fluorescence was measured by flow cytometry. Note an increase in γH2AX IF occurring in all phases of the cell cycle, after the treatment (B). The plot in C shows the percent increase in mean γH2AX IF of the cells treated with different concentration of MTX for 2 h, over the mean values of γH2AX IF of the untreated (Ctrl) cells, in the respective cell cycle phase, compensated to account for the increased DNA and histone content in S- and G_2/M-, compared to G_1-, cells (see Materials and Methods). Similar to the case of TPT-treatment (see Fig. 2), S-phase cells selectively undergo apoptosis (D).

1.5 h (Fig. 1E and F) or 3 h (Fig. 1C and D). The nonapoptotic cells from the untreated culture show minimal γH2AX IF; they are marked with arrows in Figure 1A. The fluorescence intensity of the single apoptotic cell (about 2–4% of cells in HL-60 cultures undergo spontaneous apoptosis) in this field, compared with the nonapoptotic cells, was so strong that the photograph had to be overexposed to show both the apoptotic and nonapoptotic cells. Because of the overexposure, the γH2AX IF in the apoptotic cell appears blue-white rather than green in color. Figure 1C and D show another apoptotic cell, this time in a photograph that was properly exposed. It is quite evident that the intensity of γH2AX IF was uneven, appearing much brighter and forming a ring on the periphery of the condensed chromatin of the nuclear fragments compared to staining in their center.

Interestingly, the cytoplasmic areas not overlapping with DAPI fluorescence (DNA) in the apoptotic cells, i.e., outside of chromatin structures, are distinctly labeled with the γH2AX Ab (Fig. 1C and D). Apparently, during apoptosis, γH2AX dissociates from DNA and is translocated into the cytosol. This may be a consequence of AA DNA fragmentation.

In the case of cells treated with TPT (Fig. 1E and F), two subpopulations of cells, some strongly labeled with the γH2AX Ab, and others showing weak fluorescence (Fig. 1E, arrows) can be identified. The labeling appears to have an uneven, "dotted" pattern, which is more easily discerned in the cells that do not have very strong labeling. The cells showing strong γH2AX IF were generally larger than the weakly labeled ones (Fig. 1E and F).

The scattergrams shown in Figures 2 and 3 (parts A and B, in both figures) reveal the cell cycle phase specificity of γH2AX IF following HL-60 cell treatment with TPT and MTX, respectively. The slopes of the line plots in Figures 2C and 3C illustrate the relationship between drug concentration and induction of the γH2AX IF with respect to the cell cycle phase. It is apparent that the increase in γH2AX IF in response to TPT treatment was the most pronounced in S-phase cells. In contrast, following MTX treatment, the highest increase in γH2AX IF was manifest in G_1 phase cells. The population of S phase cells, however, was the population that preferentially underwent apoptosis, as detected by the TUNEL assay (Figs. 2D and 3D) in both sets of cultures, regardless of whether they were treated with TPT or MTX.

In the next set of experiments using the multiparameter LSC and iCyte, we correlated, in the same cells, induction of γH2AX with the activation of caspase-3, chromatin condensation and cell cycle phase (Figs. 4–6). Figure 4 shows images of HL-60 cells treated with TPT for 3 h that were differentially immunostained for γH2AX and activated caspase-3 (green fluorescence), while their DNA was counterstained with DAPI. It is quite evident that the cells expressing activated caspase-3 have very strong γH2AX IF. In contrast, the cells with weak γH2AX IF are caspase-3 negative. Large numbers of cells are both caspase-3 and γH2AX negative.

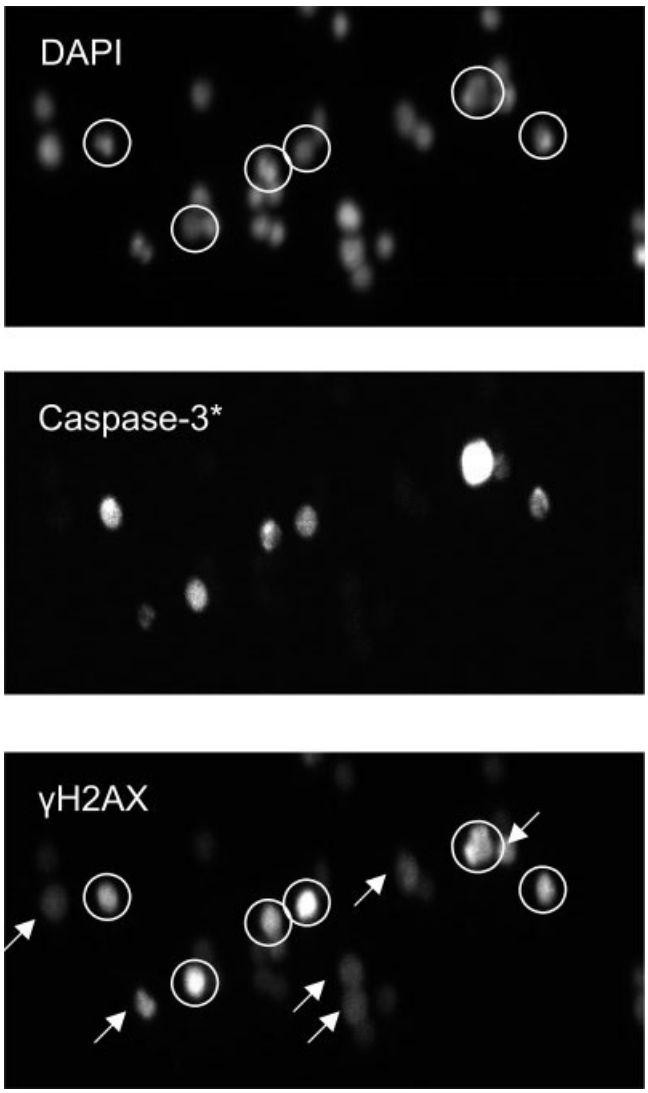

FIG. 4. iCyte-recorded black/white images of HL-60 cells treated with 0.15 μM TPT for 3 h and differentially immunostained for γH2AX (far-red fluorescence) and activated caspase-3 (green fluorescence); their DNA was stained with DAPI (blue fluorescence). Note that the cells with activated caspase-3 have very strong γH2AX IF (marked by circles). The cells expressing low level of γH2AX IF (marked by the arrows) show no expression of activated caspase-3.

Figure 5 presents the results of an experiment in which γH2AX IF of HL-60 cells, grown in the absence or presence of TPT for 1 and 3 h, was measured by multiparameter LSC, concurrent with DNA content and activation of caspase-3. Thus, activation of caspase-3 could be quantitatively correlated with induction of γH2AX in the same cells, both in relation to cell cycle position. It is quite evident that a subpopulation of predominantly S phase cells showed a moderate increase in γH2AX IF after 1 h of the treatment. As expected, there was no evidence of apoptosis as manifested by caspase-3 activation at that time. A distinct population of cells strongly expressing γH2AX IF (Ap; Fig. 5, bottom left panel) arose after 3 h

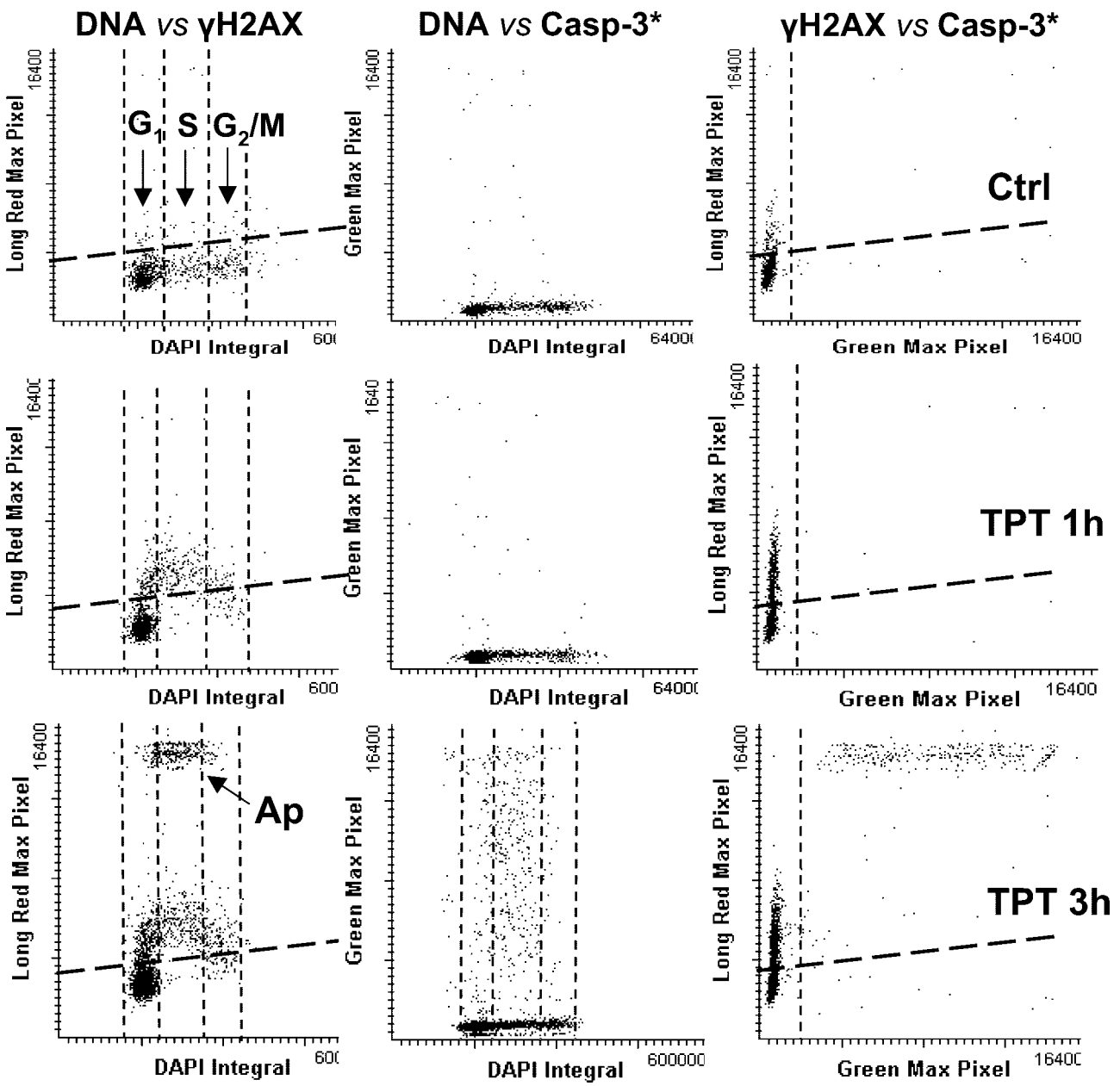

FIG. 5. Correlation between induction of γH2AX, caspase-3 activation, and cell cycle position in HL-60 cells treated with 0.15 μM TPT for 1 or 3 h. The respective scatterplots show the bivariate distributions of cellular DNA content versus induction of γH2AX, DNA content versus caspase-3 activation, and γH2AX IF versus caspase-3 activation. Each of these parameters was measured using fluorochrome of a different color (γH2AX, long-red, maximal pixel; DNA, DAPI, blue, integral; caspase-3*, green) that was excited by different laser, and fluorescence was measured by LSC, as described in Materials and Methods. The thresholds (dashed lines) represent levels of the γH2AX IF and of activated caspase-3 below which 95% and 98% of the untreated (Ctrl) cells expressed these markers, respectively.

treatment with TPT, concomitant with the appearance of cells expressing caspase-3 activation (Fig. 5, bottom middle panel). The majority of both γH2AX- and activated caspase-3-expressing cells had an S phase DNA content. By using gating analysis of γH2AX IF and caspase-3 activation, it is evident that nearly all cells demonstrating strong γH2AX IF also had activated caspase-3, i.e., they were undergoing apoptosis. In contrast, relatively few cells that showed a moderate increase in γH2AX IF contained activated caspase-3 (Fig. 5, bottom right).

The direct relationship between expression of γH2AX IF versus caspase-3 activation versus chromatin condensation, all in turn related to the cell cycle position, is illustrated in Figure 6. In this experiment, HL-60 cells were treated with TPT for 3 or 4 h, to examine possible differences between the early apoptotic cells, which prevail

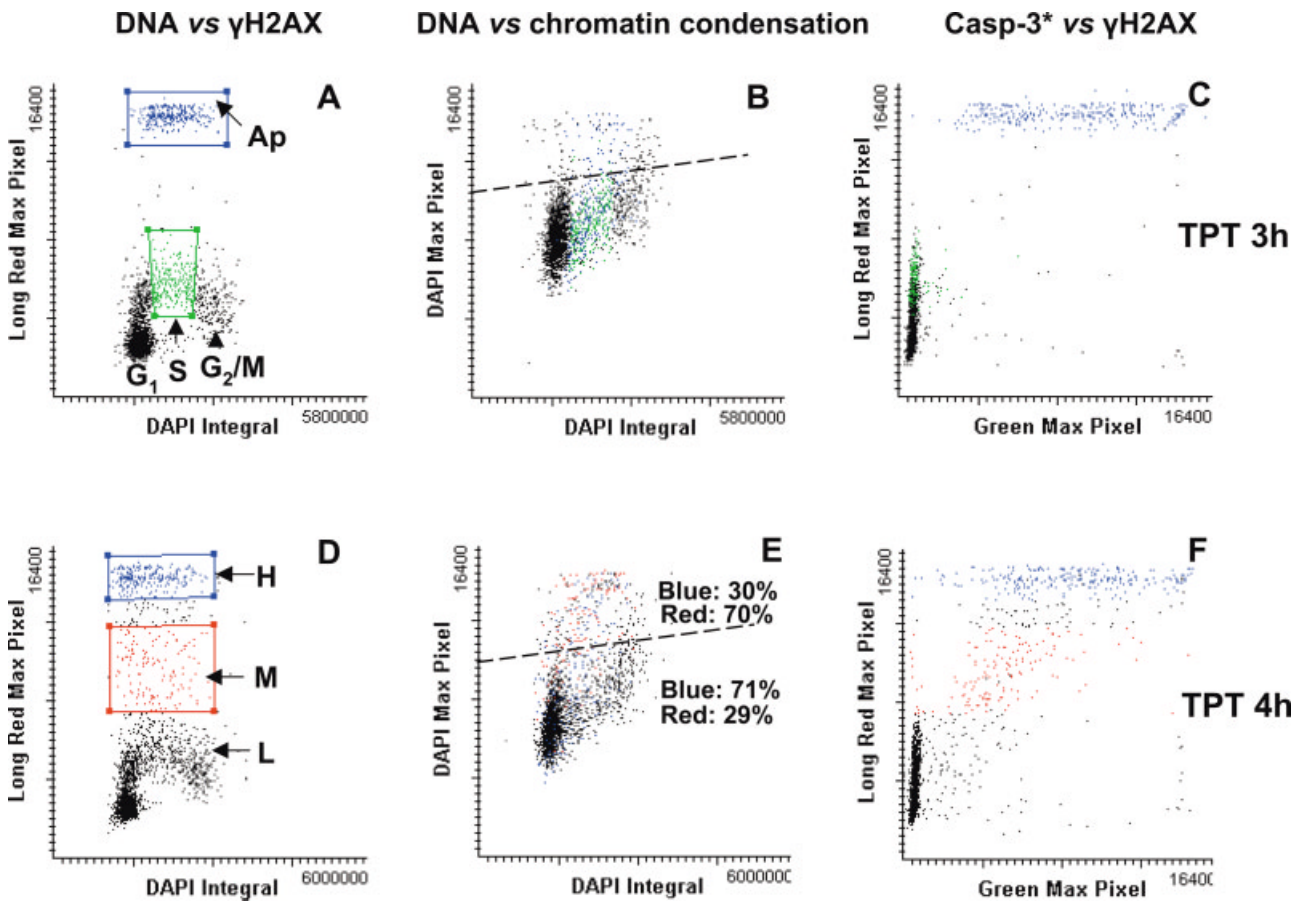

FIG. 6. Differences in intensity of γH2AX IF in relation to induction of DSBs by TPT, caspase-3 activation, and early- and late-stage of apoptosis. Exponentially-growing HL-60 cells were treated with 0.15 μM TPT for 3 h (**A–C**) or 4 h (**D–F**). γH2AX was immunostained to fluoresce in long-red wavelength (maximal pixel was recorded), caspase-3* to fluoresce in green (maximal pixel), DNA in blue (DAPI, integral), using three-laser excitation by LSC, as described in Materials and Methods. In scatterplots shown in top panels (A–C) the cells expressing maximal γH2AX IF are marked blue, the cells showing low increase in γH2AX IF are marked green. Note that essentially all blue-marked cells have activated caspase-3 (C), indicating that the cells with maximal expression of γH2AX are in process of apoptosis (Ap). A population of cells with moderate (M) expression of γH2AX IF is apparent after 4 h treatment with TPT (red-marked; D). The "paint-a-gate" analysis indicates that among the cells with the increased DAPI maximal pixel (above the arbitrary threshold marked by dashed line; E) predominate the cells with moderate expression of γH2AX IF (70%). In contrast, most cells with high (H) expression of γH2AX IF do not show the increase in intensity of maximal pixel of DAPI fluorescence. Note that the cells with moderate expression of γH2AX IF (red) also have decreased expression of activated caspase-3 compared with the cells maximally expressing γH2AX IF (F). Progression of apoptosis, which is marked by the increase in chromatin condensation (increased maximal pixel of DAPI fluorescence), thus, is accompanied by the decrease in expression of both γH2AX and of activated caspase-3.

after 3 h of treatment with TPT, and the late-apoptotic cells, which appear with increased length of exposure (4 h). Condensation of chromatin, known to occur during apoptosis (35,41), manifests as increased hyperchromicity of DNA, which in turn is detected by LSC as increased maximal pixel (i.e., concentration) of DNA-associated (DAPI) fluorescence (42,43). The gating analysis shown in the top panels of Figure 6 revealed that the cells strongly expressing γH2AX IF (Ap; marked in blue in Fig. 6A and D), all had activated caspase-3 (Fig. 6C). After 4 h treatment with TPT, a population of cells with intermediate expression of γH2AX became apparent (marked in red in Fig. 6D). Concurrently, there was an increase in the number of cells with elevated values of DAPI (blue) maximal pixel fluorescence (Fig. 6E). The gating analysis revealed that among the cells with increased DAPI maximal pixel fluorescence (above an arbitrary threshold marked with a dashed line in Fig. 6E) there was a higher percentage of cells with intermediate γH2AX IF (marked in red) than with maximal γH2AX IF (blue; 70% versus 30%). This proportion is reversed among the cells that do not yet show increased chromatin condensation, i.e., with maximal pixel values of DAPI-fluorescence below the threshold indicated in Figure 6. Thus, in the later stages of apoptosis (characterized by increased levels of chromatin condensation), a decrease in γH2AX IF was observed. Interestingly, the progression of apoptosis was also paralleled by a decrease in expression of activated caspase-3. This was evident by the fact that the cells with moderate expression of γH2AX (red) also had distinctly lower expression of activated caspase-3 compared with the blue-marked cells (Fig. 6F).

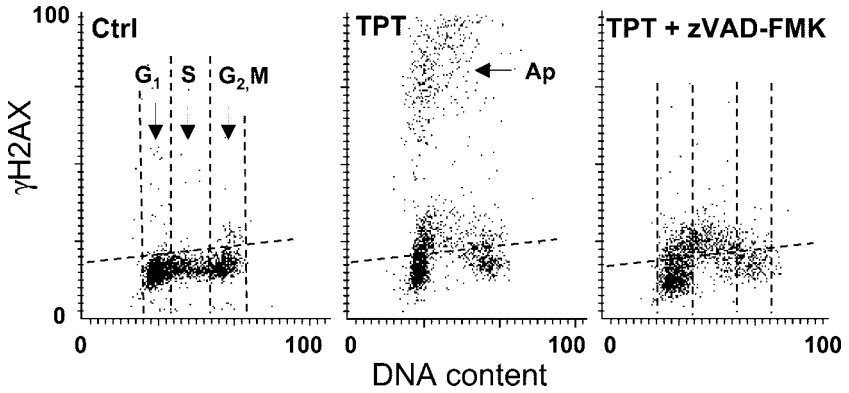

FIG. 7. Effect of pan-caspase inhibitor z-VAD-FMK on γH2AX IF following treatment with TPT. HL-60 cells were left untreated (Ctrl) or were treated with 150 nM of TPT in the absence or presence of 50 μM of z-VAD-FMK for 3 h. The dashed horizontal line represents the threshold below which 95% cells from the untreated (Ctrl) culture expresses γH2AX. Note that the TPT-induced appearance of cells with strong γH2AX IF (Ap), but not of the cells with low level of γH2AX IF, was prevented by zVAD-FMK.

Administration of the pan-caspase inhibitor z-VAD-FMK concurrent with the cell treatment with TPT precluded the appearance of cells strongly expressing γH2AX (Fig. 7). It did not affect, however, the low level of induction of γH2AX IF by S and a fraction of G_1 cells.

In the presence of phosphatase inhibitor calyculin A (44), the TPT-induced increase in γH2AX IF was little affected after 1 h of the treatment, but was markedly higher 3 h after administration of the drug (Fig. 8). After the subtraction of γH2AX IF due to the "programmed" H2AX phosphorylation represented by the untreated (Ctrl) cells, the mean intensity of γH2AX IF was 3.4-, 3.2-, or 2.7-fold higher for the population of G_1, S, or G_2/M cells compared to the cells treated with TPT alone in the same phases of the cell cycle, respectively.

We also tested whether the antitumor drug that does not directly induce DSBs can affect the expression of H2AX. Such a drug is CP, which is known to generate the DNA intrastrand, and to a lesser degree interstrand cross-links, but no DSBs as the primary lesions (31,32). Following 1 h treatment with CP, a rather small percentage of cells (<16%) showed γH2AX IF elevated above the control level (Fig. 9). After 3 h, however, the numbers of cells with the increased γH2AX IF was quite substantial, particularly at 1.0 or 2.0 μM concentration of this drug (Fig. 9). However, there was no evidence of the cell cycle–phase specificity in the increase γH2AX IF following treatment with CP.

DISCUSSION

We have recently reported (33) that exposure of HL-60 cells to DNA topo1 (camptothecin or TPT), or topo2 (MTX) inhibitor leads to an increase in binding of the γH2AX Ab by the treated cells. This Ab is specific towards

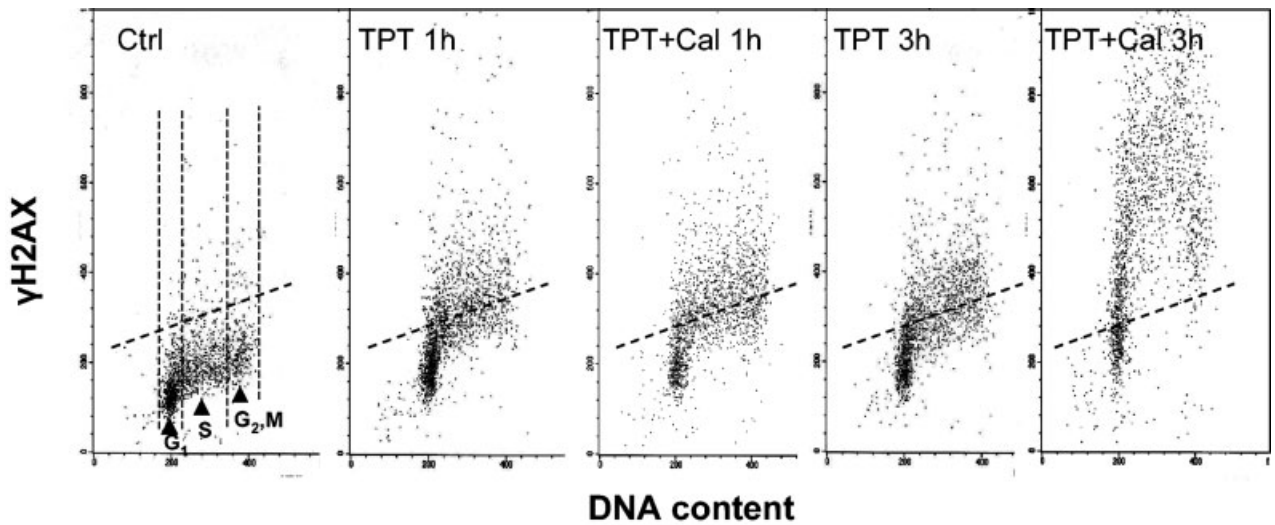

FIG. 8. Effect of calyculin A on expression of γH2AX in HL-60 cells cultured in the presence of TPT. The bivariate distributions of γH2AX expression in relation to cellular DNA content (cell cycle position) of untreated HL-60 cells (Ctrl) and cells cultured with 0.15 μM of TPT in the absence and presence of 10 nM calyculin A (Cal) for 1 or 3 h. Notice no significant effect of calyculin A on expression of γH2AX after 1 h treatment with TPT, but marked increase in the expression of γH2AX (apparent in all phases of the cell cycle) after 3 h, compared to the culture treated with TPT in the absence of calyculin A. The dashed horizontal line represents the γH2AX IF level below which over 95% of cells from the untreated culture (Ctrl) express γH2AX. By gating analysis, the mean values of γH2AX IF for cell populations in G_1, S, and G_2/M were estimated in control, TPT, and TPT+calyculin A treated cultures. While no significant effect of calyculin A was seen after 1 h, after 3 h the mean γH2AX IF of cells exposed to TPT+calyculin A was 2.7- to 3.4-fold higher compared to cells treated with TPT alone.

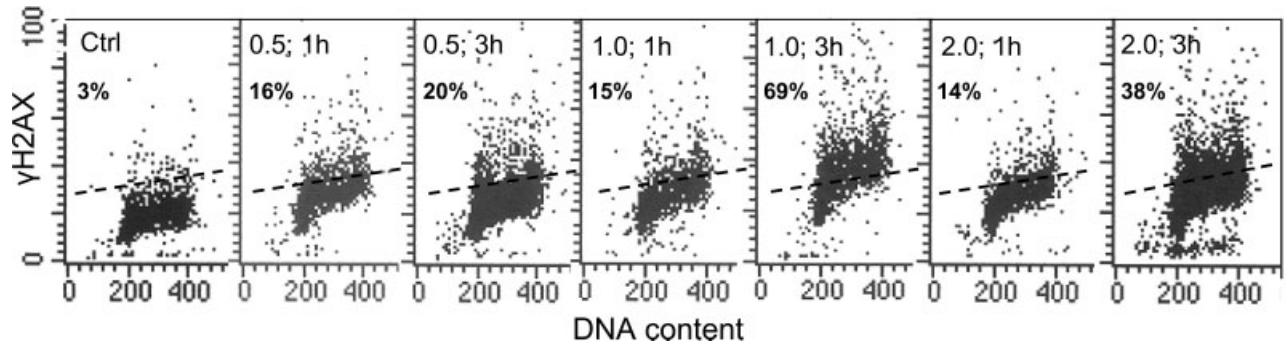

FIG. 9. Expression of γH2AX in HL-60 cells treated of cisplatin (CP). The scatterplots show bivariate distributions of γH2AX IF versus DNA content of HL-60 cells treated with 0.5, 1.0, or 2.0 μM CP for 1 h or 3 h. The dashed line represents the arbitrary level of γH2AX IF; the percent of cells expressing γH2AX IF above this level is indicated in each panel. The cells treated with CP for 3 h, especially at 1.0 and 2.0 μM concentration, have higher intensity of γH2AX IF compared to cells treated for 1 h. No cell cycle–phase specificity in expression of γH2AX is apparent.

the H2AX phosphorylated on Ser-139, and its binding by permeabilized cells, therefore, is being considered to report histone phosphorylation. Phosphorylation of H2AX was shown to occur in response to induction of DSB in chromatin by ionizing radiation (21–24), and, as mentioned, in the case of topo1 or topo2 inhibitor-treated cells, DSB are generated by collisions between the progressing replication fork or RNA polymerase complex, and the topo1 or topo2 stabilized cleavable complex (25–27). The multiparameter flow or laser-scanning cytometry that combines immunocytochemical detection of γH2AX with other parameters such as cell cycle phase, caspase-3 activation, or chromatin condensation, thus, offers a convenient tool to study DNA damage by these inhibitors. Such an approach has been recently used to investigate DSB induced by ionizing radiation (21,23,24).

Confirming the observations of McPhail et al. (21), we observed a low level of γH2AX IF in untreated HL-60 cells (Fig. 1). The untreated Jurkat and transitional cell carcinoma T24 cells showed low intensity γH2AX IF as well (not shown). In addition, the foci of γH2AX IF in the untreated cells were of a smaller size than in the drug-treated ones, also in agreement with the observation of these authors (21). For quantitative analysis of DI γH2AX IF, this programmed (or scheduled) level of histone H2AX phosphorylation, which appears to be primarily associated with DNA replication (21), was subtracted from the mean values of the drug treated cells, for each cell cycle phase, separately. Thus, the plots in Figures 2C and 3C represent the DI increase in γH2AX immunofluorescence, for each phase of the cell cycle (see Material and Methods). This increase is expressed as percent of the IF of the untreated cells in the same phase of the cycle.

Histone content doubles during the cell cycle along with the doubling of DNA. Unlike other proteins, however, whose content may vary in individual cells with respect to DNA content, histone synthesis is coupled with DNA synthesis and therefore the ratio of histone to DNA content remains invariable throughout the cell cycle for all cells (44). As a consequence of their higher histone content, therefore, with the same degree of H2AX phosphorylation (the same percent of phosphorylated H2AX molecules within the total H2AX molecules), the cells in S and G_2/M have 1.5 and 2.0 times higher γH2AX IF compared to cells in G_1. To assess the degree of H2AX phosphorylation, and thus to make γH2AX IF independent of histone doubling during the cycle, we have normalized the data by presenting them per unit of DNA (histone). This was accomplished by multiplying the mean S-phase and G_2/M-phase γH2AX IF of the untreated cells as well as the Δ-γH2AX of the drug-treated cells, by 0.75 and 0.5, respectively (Figs. 2C and 3C). The data shown in these plots, thus, represent not the cellular content of γH2AX in relation to the cell cycle, but after compensating for the change in total H2AX content, the degree of H2AX phosphorylation, representing a ratio of phosphorylated H2AX molecules per total number of H2AX within each cell. In fact, because the background fluorescence, i.e. the fluorescence of the untreated cells, was subtracted, per population of G_1, S, or G_2/M cells, respectively, the ΔγH2AX IF shown on these plots represents the DI increase in the degree of H2AX phosphorylation.

The following attributes allow one to distinguish the cells with DI H2AX phosphorylation from the cells that have an additional, phosphorylation of this histone, triggered by DNA fragmentation during apoptosis: 1) The DI γH2AX IF is seen very early (during the initial two hours) during the treatment, i.e., well prior to caspase-3 activation, which is the prerequisite for the apoptotic endonuclease activation and DNA fragmentation (34). 2) The intensity of DI γH2AX IF is several-fold lower than the intensity of AA γH2AX IF (Fig. 5). It should be noted, however, that because the intensity of the AA γH2AX IF decreases during progression of apoptosis (Fig. 6), at late stages of apoptosis this attribute may fail to discriminate between DI- versus AA-γH2AX IF. 3) The difference in sensitivity of AA versus DI phosphorylation of histone H2AX to the caspase inhibitor zVAD-FMK; in its presence only DI γH2AX is detected (Fig. 7). 4) The AA H2AX phosphorylation occurs in parallel with the concurrent activation of caspase-3 in the same cells. Multiparameter (activated caspase-3 versus γH2AX IF) cytometry, thus,

appears to be the most direct approach to distinguish the cells in which DNA strand breaks (histone H2AX phosphorylation) were induced by the studied drugs, from the cells that have H2AX phosphorylation additionally triggered in response to apoptotic DNA fragmentation.

There is an equilibrium between the rate of phosphorylation of histone H2AX after DNA damage, and its dephosphorylation that occurs when DNA repair progresses (45). We observed that the intensity of γH2AX IF was elevated when the cells were treated with TPT in the presence of the protein (serine/threonine) phosphatase inhibitor calyculin A for 3 h but was essentially unchanged after 1 h of the treatment. These data indicate that while no significant dephosphorylation of H2AX occurs during the first hour of treatment, significant degree of dephosphorylation occurs between 1 and 3 h. Our data conform with the observation of Nazarov et al. (45), who reported that following DNA damage by ionizing radiation 50% of H2AX is already dephosphorylated after 3 h. In fact, by comparing the mean values of γH2AX IF of the cells treated with TPT in the presence and absence of calyculin A for 3 h (Fig. 8), one may conclude that dephosphorylation of H2AX during TPT treatment, at a 3-h time interval, was even more extensive (3.4- to 2.7-fold) than after ionizing radiation, as observed by Nazarov et al. (45). To obtain a measure of the cumulative H2AX phosphorylation (as a yardstick of the total number of DSBs) in response to progressive DNA damage (e.g., as occurs during continuous cell treatment with a DNA damaging drug), one has to incubate the cells in the presence of the protein phosphatase inhibitor, to prevent γH2AX dephosphorylation. It should be noted, however, that calyculin A is cytotoxic and prolonged (>3 h) cell incubation with this inhibitor leads to extensive chromatin condensation followed by apoptosis (unpublished results).

A plateau and a decline in the intensity of γH2AX IF was seen at the higher ranges of concentration of TPT or MTX (Figs. 2 and 3). It is possible that at high concentration these intercalating drugs alter DNA topology by inducing torsional stress on double helical DNA in the closed loops of chromatin (46). Such a change is expected to inhibit progression of the replication forks or RNA polymerase molecules along the DNA molecule, thereby lowering the incidence of their collisions with the cleavable complexes and induction of DSB.

The pattern of response of HL-60 cells to the topo1 inhibitor TPT versus the topo2 inhibitor MTX vis-à-vis cell cycle position was distinctly different. Namely, whereas TPT induced H2AX phosphorylation preferentially in S-phase cells, this selectivity was not apparent in the case of MTX treated cells. In fact, after compensation for the increase in total histone content that occurs during S, the G_1 cells demonstrated a higher degree of H2AX phosphorylation than S or G_2/M cells after exposure to MTX. Yet, the S-phase cells preferentially underwent apoptosis after treatment with MTX (Fig. 3). This data indicates that, at least in the case of treatment with MTX, notwithstanding the same or even lower frequency of DSB, DNA replicating cells are more prone to undergo apoptosis than G_1 or G_2/M cells. It appears, therefore, that with a comparable extent of DNA damage, the cells arrested at the G_1 or G_2/M checkpoint remain at the checkpoint alive for extended period of time, apparently in an attempt to repair the damage, while the S-phase cells succumb to apoptosis.

We observed the increase in phosphorylation of H2AX following the cell treatment with CP, which was more pronounced 3 h after drug administration than after 1 h (Fig. 9). The CP-induced H2AX phosphorylation cannot be attributed to apoptosis, because during the initial 3 h of the treatment no caspase activation was detected (data not shown). Furthermore, the AA rise in γH2AX IF is of much higher degree (Fig. 5) than that observed after treatment (Fig. 8). The observed increase in γH2AX IF in cells treated with CP, thus, was definitely drug-induced. However, in contrast to topo inhibitors, CP cross-links DNA rather than induces DSB (31,32). It is unlikely, therefore, that the primary lesions induced by CP (DNA cross-links), contributed to the observed H2AX phosphorylation. The repair process of these lesions, however, involves the NER mechanism, known to generate ss DNA breaks. A fraction of ss DNA breaks, in turn, is known to be converted in the cell to ds DNA breaks (47). Furthermore, repair of cisplatin-induced damage also involves NHEJ (48). This mechanism may additionally contribute to the formation of ds DNA breaks and to the observed H2AX phosphorylation. Thus, when the primary drug-induced lesions do not involve ds DNA breaks, but ds DNA breaks are formed during DNA repair, as in the case of CP, analysis of H2AX phosphorylation may indicate efficiency of the repair process.

REFERENCES

1. West MH, Bonner WM. Histone 2A, a heteromorphous family of eight protein species. Biochemistry 1980;19:3238–3245.
2. Thatcher TH, Gorovsky MA. Phylogenetic analysis of the core histones H2A, H2B, H3 and H4. Nucleic Acids Res 1994;22:174–179.
3. Pehrson JR, Fuji RN. Evolutionary conservation of histone macro-H2A subtypes and domains. Nucleic Acids Res 1998;26:2837–2842.
4. Rogakou EP, Pilch DR, Orr AH, Ivanova VS, Bonner WM. DNA double-stranded breaks induce histone H2AX phosphorylation on serine 139. J Biol Chem 1998;273:5858–5868.
5. Sedelnikova OA, Rogakou EP, Panuytin IG, Bonner W. Quantitive detection of 125IUdr-induced DNA double-strand breaks with γ-H2AX antibody Radiat Res 2002;158:486–492.
6. Burma S, Chen BP, Murphy M, Kurimasa A, Chen DJ. ATM phosphorylates histone H2AX in response to DNA double-strand breaks. J Biol Chem 2001;276:42462–42467.
7. Anderson L, Henderson C, Adachi Y. Phosphorylation and rapid relocalization of 53BP1 to nuclear foci upon DNA damage. Mol Cell Biol 2001;21:1719–1729.
8. Furuta T, Takemura H, Liao-Z-Y, Aune GJ, Redon C, Sedelnikova OA, Pilch DR, Rogakou EP, Celeste A, Chen HT, Nussenzweig A, Aladjem MI, Bonner WM, Pommier Y. Phosphorylation of histone H2AX and activation of Mre11, Rad50, and Nbs1 in response to replication-dependent DNA double-strand breaks induces by mammalian topoisomerase I cleavage complexes. J Biol Chem 2003;278:20303–20312.
9. Park EJ, Chan DW, Park JH, Oettinger MA, Kwon J. DNA-PK is activated by nucleosomes and phosphorylated H2AX within the nucleosomes in an acetylation-dependent manner. Nucleic Acids Res 2003;31:6819–6827.
10. Rogakou EP, Boon, C, Redon, C, Bonner WM. Megabase chromatin domains involved in DNA double-strand breaks *in vivo*. J Cell Biol 1999;146:905–916.
11. Paull TT, Rogakou EP, Yamazaki V, Kirchgesser CU, Gellert M, Bonner WM. A critical role for histone H2AX in recruitment of repair factors to nuclear foci after DNA damage. Curr Biol 2000;10:886–895.
12. Celeste A, Fernandez-Capetillo O, Kruhlak MJ, Pilch DR, Staudt DW,

Lee A, Bonner RF, Bonner WM, Nussenzweig A. Histone H2AX phosphorylation is dispensable for the initial recognition of DNA breaks. Nat Cell Biol 2003;5:675–679.
13. Celeste A, Paterson S, Romanienko PJ, Fernandez-Capetillo O, Chen HT, Sedelnikov OA, Reina-San-Martin B, Coppola V, Meffre E, Difilippantonio MJ, Redon C, Pilch DR, Olaru A, Eckhaus M, Camerini-Otero RD, Tessarollo L, Livak F, Manova K, Bonner WM, Nussenzweig MC, Nussenzweig A. Genomic instability in mice lacking histone H2AX. Science 2002;296:922-927.
14. Celeste A, Difilippantonio S, Fernandez-Capetillo O, Pilch DR, Sedelnikova O, Eckhaus M, Ried T, Bonner WM, Nussenzweig A. H2AX haploinsufficiency modifies genomic stability and tumor susceptibility. Cell 2003;114:371–383.
15. Bassing CH, Suh H, Ferguson DO, Chua KF, Manis J, Eckersdorff M, Gleason M, Bronson R, Lee C, Alt FW. Histone H2AX: a dosage-dependent suppressor of oncogenic translocations in tumors. Cell 2003;114:359–370.
16. Downs JA, Lowndes NF, Jackson SP. A role for *Saccharomyces cerevisiae* histone H2A in DNA repair. Nature 2000;408:1001–1004.
17. Jackson SP. DNA damage signaling and apoptosis. Biochem Soc Trans 2001;29:655–661.
18. Fernandez-Capetillo O, Chen H-T, Celeste A, Ward I, Romanienko P, Morales JC, Naka K, Xia Z, Camerini-Otero RD, Motoyama N, Carpenter PB, Bonner WM, Chen J, Nussenzweig A. DNA damage-induced G_2-M checkpoint activation by histone H2AX and 53BP1. Nat Cell Biol 2002;4:993–997.
19. Modesti M, Kanaar R. DNA repair: spot(light)s on chromatin. Curr Biol 2001;11:R229–R232.
20. Sedelnikova OA, Pilch DR, Redon C, Bonner WM. Histone H2AX in DNA damage and repair. Cancer Biol Ther 2003;2:233–235.
21. MacPhail SH, Banath JP, Yu Y, Chu E, Olive PL. Cell cycle-dependent expression of phosphorylated histone H2AX: reduced expression in unirradiated but not X-irradiated G1-phase cells. Radiat Res 2003;159:759–767.
22. Yoshida K, Yoshida SH, Shimoda C, Morita T. Expression and radiation-induced phosphorylation of H2AX in mammalian cells. J Radiat Res (Tokyo) 2003;44:47–51.
23. MacPhail SH, Banath JP, YuTY, Chu EH, Lambur H, Olive PL. Expression of phosphorylated histone H2AX in cultured cell lines following exposure to X-rays. Int J Radiat Biol 2003;79:351–358.
24. Banath JP, Olive PL. Expression of phosphorylated of histone H2AX as a surrogate of cell killing by drugs that create DNA double-strand breaks. Cancer Res 2003;63:4347–4350.
25. Hsiang YH, Lihou MG, Liu LF. Arrest of replication forks by drug stabilized topoisomerase I-DNA cleavable complexes as a mechanism of cell killing by camptothecin. Cancer Res 1989;49:5077–5082.
26. D'Arpa P, Beardmore C, Liu LF. Involvement of nucleic acid synthesis in cell killing mechanisms of topoisomerase poisons. Cancer Res 1990;50:6916–6924.
27. Wu J, Liu LF. Processing of topoisomerase I cleavable complexes into DNA by transcription. Nucleic Acids Res 1997;25:4181–4186.
28. Del Bino G, Skierski JS, Darzynkiewicz Z. Diverse effects of camptothecin, an inhibitor of topoisomerase I, on the cell cycle of lymphocytic (L1210, MOLT-4) and myelogenous (HL-60, KG1) leukemic cells. Cancer Res 1990;50:5746–5750.
29. Del Bino G, Lassota P, Darzynkiewicz Z. The S-phase cytotoxicity of camptothecin. Exp Cell Res 1991;193:27–35.
30. Gorczyca W, Gong J, Ardelt B, Traganos F, Darzynkiewicz Z. The cell cycle related differences in susceptibility of HL-60 cells to apoptosis induced by various antitumor agents. Cancer Res 1993;53:3186–3192.
31. Siddick ZH. Cisplatin: mode of cytotoxic action and molecular basis of resistance Oncogene 2003;22:7265–7279.
32. Faivre S, Chan D, Salinas R, Woynarowska B, Woynarowski JM. DNA strand breaks and apoptosis induced by oxaliplatin in cancer cells. Biochem Pharmacol 2003;66:225–237.
33. Huang X, Traganos F, Darzynkiewicz Z. DNA damage induced by DNA topoisomerase I- or topoisomerase II- inhibitors detected by histone H2AX phosphorylation in relation to the cell cycle phase and apoptosis. Cell Cycle 2003;2:614–619.
34. Earnshaw WC, Martins LM, Kaufmann SH. Mammalian caspases: structure, activation, substrates and functions during apoptosis. Annu Rev Biochem 1999;68:383–424.
35. Darzynkiewicz Z, Bruno S, Del Bino G, Gorczyca W, Hotz MA, Lassota P, Traganos F. Features of apoptotic cells measured by flow cytometry. Cytometry 1992;13:795–808.
36. Kamentsky LA. Laser scanning cytometry. Methods Cell Biol 2001;63:51–83.
37. Darzynkiewicz Z, Bedner E, Li X, Gorczyca W, Darzynkiewicz Z. Laser-scanning cytometry: a new instrumentation with many applications. Exp Cell Res 1999;249:1–12.
38. Gorczyca W, Bruno S, Darzynkiewicz RJ, Gong J, Darzynkiewicz Z. DNA strand breaks occurring during apoptosis: their early *in situ* detection by the terminal-deoxynucleotidyl transferase and nick translation and prevention by serine protease inhibitors. Int J Oncol 1992;1:639–648.
39. Li X, Darzynkiewicz Z. Labelling DNA strand breaks with BrdUTP. Detection of apoptosis and cell proliferation. Cell Prolif 1995;28:571–579.
40. Li X, Darzynkiewicz Z. Cleavage of poly(ADP-ribose) polymerase measured in situ in individual cells: relationship to DNA fragmentation and cell cycle position during apoptosis. Exp Cell Res 2000;255;125–132.
41. Kerr JFR, Wyllie A, Curie AR. Apoptosis: a basic biological phenomenon with wide ranging implications in tissue kinetics. Br J Cancer 1972;26;239–257.
42. Furuya T, Kamada T, Murakami T, Kurose A, Sasaki K. Laser scanning cytometry allows detection of cell death with morphological features of apoptosis in cells stained with PI. Cytometry 1997;29:173–177.
43. Pozarowski P, Huang X, Halicka HD, Lee B, Johnson G, Darzynkiewicz Z. Interactions of fluorochrome-labeled caspase inhibitors with apoptotic cells. A caution in data interpretation. Cytometry 2003;55A;50–60.
44. Marzluff WF, Duronio RJ. Histone mRNA expression: multiple levels of cell cycle regulation and important developmental consequences. Curr Opin Cell Biol 2002;14:692–699.
45. Nazarov IB, Smirnova AN, Krutilina RI, Svetlova MP, Solovjeva LV, Nikiforov AA, Oei S-L, Zalenskaya IA, You PM, Bradbury EM, Tomilin NV. Dephosphorylation of histone γ-H2AX during repair of DNA double-strand breaks in mammalian cells and its inhibition by calyculin A. Radiat Res 2003;160:309–317.
46. Ralph RK, Hancock R. Chromosomal DNA fragments from mouse cells exposed to an intercalating agent contain a 175-kdalton polypeptide. Can J Biochem Cell Biol 1985;63:780–783.
47. Vilenchik MM, Knudson AG. Endogenous DNAdouble-strand breaks: production, fidelity of repair, and induction of cancer. Proc Natl Acad Sci USA 2003;100:12871–12876.
48. Crul M, van Waardenburg RCAM, Bocxe S, van Eijndhoven MAJ, Pluim D, Beijnen JH, Schellens JHM. DNA repair mechanisms involved in gemcitabine cytotoxicity and in the interaction between gemcitabine and cisplatin. Biochem Pharmacol 2003;65:275–282.